# EXAFS study of size dependence of atomic structure in palladium nanoparticles

Vasiliy V. Srabionyan [a], Aram L. Bugaev [a], Vasiliy V. Pryadchenko [a], Leon A. Avakyan [a], Jeroen A. van Bokhoven [b,c], Lusegen A. Bugaev [a,*]

[a] Physical Department, Southern Federal University, Zorge street 5, Rostov-on-Don 344090, Russia
[b] ETH Zurich, Institute for Chemical and Bioengineering, ETH, HCI E127, 8093 Zurich, Switzerland
[c] Laboratory for Catalysis and Sustainable Chemistry, SLS, Paul Scherrer Institute, 5232 Villigen, Switzerland

## ARTICLE INFO

## ABSTRACT

Dependence of atomic structure of Palladium nanoparticles on supports $Al_2O_3$ and $SiO_2$ upon their size, changed from 1.3 to 10.5 nm, was studied by Pd K-edge EXAFS. To determine the structure of the interior (core) and the near surface regions of nanoparticle, the fitting technique of the Fourier-transforms $F(R)$ of spectra was used, which enabled to overcome instabilities of the obtained structural parameters values. The processing of experimental data was performed using results of the study of features formation in $|F(R)|$ of Pd K-EXAFS in Pd foil. By this approach it was revealed that the local structure of Pd atoms in the core is similar to fcc structure of bulk Pd, irrespective of size. The percentage of Pd atoms, which can be attributed to the core, upon the particles size was determined and the obtained dependence was described by the "cluster size equation". In the near surface region of nanoparticles, nearest-neighbors Pd–Pd distances show a large Debye–Waller parameters and the mean bond length slightly contracted for nanoparticles of sizes less than $\sim$2 nm. The effect of small structural distortions in the vicinity of absorbing Pd atom in the near surface region was studied using the cluster model of nanoparticle.

## 1. Introduction

Noble metal nanoparticles find wide application in catalysis and electrochemistry [1–6] because they have several advantageous above the corresponding bulk compounds, foremost, because of their large surface area. The structure and atomic composition of the near-surface region and the amount of exposed active sites determine the catalytic properties. Therefore, the atomic structure of noble metal nanoparticles, the dependence of this structure on the treatment conditions, the supports and the particle size are extensively studied to obtain the structure-performance relationship, essential to design better catalysts [7–14]. X-ray absorption spectroscopy (XAS) is one of the most effective methods for structural analysis since experimental spectra of nanoparticles, differently prepared or attached to different supports, differ essentially from the spectra of corresponding bulk compounds. Interpretation of the observed differences in spectra and their numerical analysis enables one to get structural information of nanoparticles.

In this paper, XAS is applied to determine the atomic structure in naked Palladium nanoparticles of different size with diameter ($D$) varying from 1.3 to 10.5 nm and supported on $Al_2O_3$ and $SiO_2$.

Palladium nanoparticles are extensively used to solve various ecological problems as catalyst converters for afterburning of noxious components of exhausts, in hydrogen energetic, and therefore, they have been studied by different experimental and theoretical methods, including XAS [15–25]. However, the structural information dominantly had an averaged (over the interior or core and surface regions of nanoparticle) character. Moreover, the two following problems in the size dependence of nanoparticles structure still remain challenging: (i) there is no consensus in the literature data if the average nearest-neighbor Pd–Pd distance reduces or remains constant with a decrease of particles size and (ii) what is the point symmetry type in the core region of small metallic Palladium nanoparticles with size less than $\sim$3 nm.

To get structural information of the interior and near-surface regions of Palladium nanoparticles the analysis based on the fitting technique of the Fourier-transforms $F(R)$ of experimental Pd K-edge extended x-ray absorption fine structure (EXAFS) was performed. The application of this approach, even in the simple assumption of homogeneous structure of nanoparticle, leads to a large number of fit variables, which are often strongly correlated. The results of the fit of $F(R)$ depend also upon the wave numbers interval $\Delta k = k_{max} - k_{min}$, used for the Fourier-transformation (FT) of the oscillatory part $\chi(k)$ of experimental EXAFS, and hence $\Delta k$ must be considered as one of the factors, which affects the outcome. As a result, the fitting procedure becomes unstable and normally

* Corresponding author. Tel.: +7 863 297 53 36, fax: +7 863 297 51 20..
E-mail address: bugaev@sfedu.ru (L.A. Bugaev).

gives only the average values of a limited number of structural parameters. In Section 2 the scheme of FT of experimental spectra and the fitting technique of their $F(R)$ are presented which enabled to reduce instabilities of the fit, uncertainties in the determined values of parameters and to overcome the mentioned difficulties in the structural analysis of metallic Palladium nanoparticles on $Al_2O_3$ and $SiO_2$ as supports by Pd K-edge EXAFS. In Section 3 the fitting technique is applied to determine the atomic structure of the core region of Palladium nanoparticles, the percentage of Pd atoms in that core, the mean values of the structural parameters for Pd atoms in the near-surface region and the dependencies of these parameters upon the particles size.
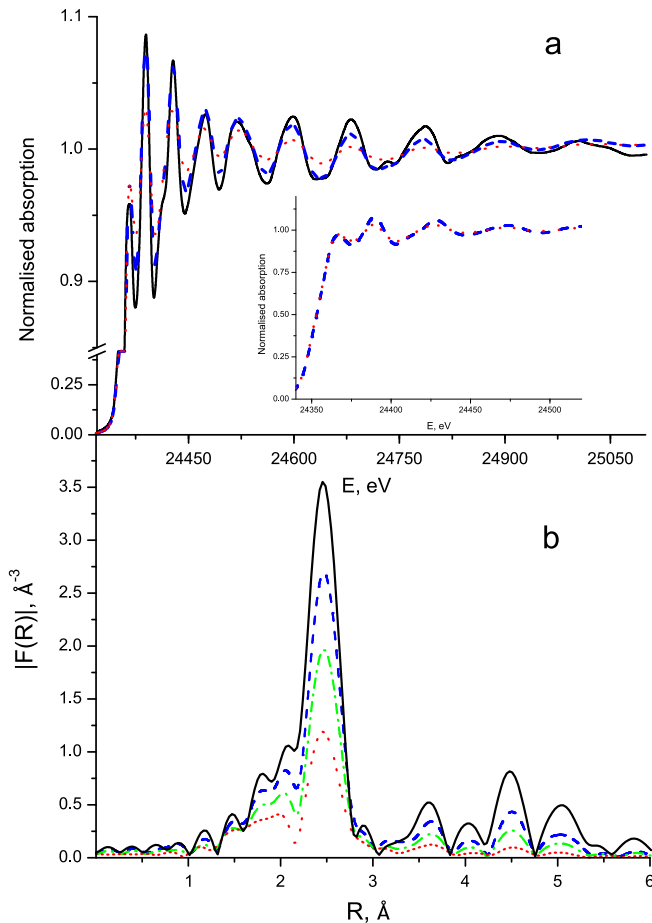


**Fig. 1.** Experimental Pd K-edge XAFS spectra (a) and corresponding FT magnitudes $|F(R)|$ of $k^2\chi(k)$ (b), obtained by the $\Delta k$ interval with $k_{min}=2.5$ Å$^{-1}$, $k_{max}=14.0$ Å$^{-1}$: in Pd foil (solid black curves) and in naked Palladium nanoparticles of different sizes: $D=10.5$ nm (dashed blue curves), $D=2.8$ nm (dash–dotted green curves) and $D=1.3$ nm (dotted red curves). The inset in (a) enlarges the low-energy region of the spectra of nanoparticles. (For interpretation of the references to color in this figure legend, the reader is referred to the web version of this article.)

## 2. The data analysis method

Experimental Pd K-edge XAFS spectra of naked Palladium nanoparticles of different size and supported on $Al_2O_3$ and $SiO_2$ were recorded in [26]. In Fig. 1, experimental Pd K-edge XAFS and their Fourier-transforms $F(R)$ of $k^2\chi(k)$, obtained by the $\Delta k$ interval with $k_{min}=2.5$ Å$^{-1}$, $k_{max}=14.0$ Å$^{-1}$, for the smaller sizes ($D=1.3$ and 2.8 nm) and for the largest size ($D=10.5$ nm) are compared with Pd K-edge XAFS in metallic Pd foil. Normalization of experimental spectra was performed using the algorithm utilized in Autobk 2.9 included in IFEFFIT package [27].

Comparison in Fig. 1(a) shows that there are no significant changes in energy position of experimental Pd K-edges and of the peaks, beginning from the first near edge one, except for the small ($<1$ eV) shifts in inflection points of spectra, which are negligible for larger particles. Therefore the functions $\chi(k)$ of the foil and of nanoparticles were obtained in the same k-scale with the zero at the inflection point $E_0=24357.5$ eV. The amplitudes of the XAFS oscillations in the spectra of nanoparticles are lower with decreasing of size, reducing the k-interval of the signal $\chi(k)$ to $k_{max}\sim14$ Å$^{-1}$. Fig. 1(b) shows that in the extended R-range, all the peaks in $|F(R)|$ of Pd foil are present in $|F(R)|$ of all spectra of nanoparticles, but of strongly reduced intensity. For Pd foil these peaks are excellently reproduced (vide infra), taking into account the first four shells of Pd in *fcc* structure and therefore, the comparison of Fig. 1 (b) indicates the presence of *fcc* Pd local structure for at least part of Pd atoms in Palladium nanoparticles of sizes from 1.3 to 10.5 nm, thus excluding an icosahedron symmetry for the small ($D\sim1.5$ nm) nanoparticles suggested by the density functional theory (DFT) modeling [24].

The behavior of experimental Pd K-edge XAFS is reflected in the results of the fit of Fourier-transforms $F(R)$ of $k^2\chi(k)$ of these spectra, obtained by the $\Delta k$ interval with $k_{min}=2.5$ Å$^{-1}$, $k_{max}=14.0$ Å$^{-1}$ using code FEFFIT [27] and assuming that Pd local structure in Pd-foil and in the nanoparticles can be represented by a single-term contribution (Table 1). The inclusion of cumulants expansion [28] in the fit of $F(R)$ of Pd foil, used as a reference compound, yielded $C_3\approx C_4\approx0.0$ and did not change the values of structural parameters, which indicates that anharmonicity effects in Pd–Pd motion at room temperature are negligible.

Pd foil as a reference compound was used also to establish the value of the reduction factor $S_0^2$ [29]. For this purpose the correlation between $S_0^2$ and Debye–Waller (DW) parameter $\sigma^2$ was reduced using different dependencies $\{\sigma^2(S_0^2)\}_{k^n,(\Delta k)_i}$, which were obtained from the experimental Pd K-edge EXAFS in foil under differently weighted functions $k^n\chi(k)$ ($n=0, 1, 2$) and for different $\Delta k_i$ intervals ($i$ is the number of interval) for FT. The crossing region of these curves $\{\sigma^2(S_0^2)\}_{k^n,(\Delta k)_i}\cap\{\sigma^2(S_0^2)\}_{k^p,(\Delta k)_j}$ was centered at the following values of parameters: $\sigma^2=0.0058$ Å$^2$ (presented in Table 1) and $S_0^2=0.85$. This value of $S_0^2$ was used in the following study of Palladium nanoparticles atomic structure and in Table 1, where the values of $<N>$ for nanoparticles were obtained by dividing the corresponding values of variable $S_0^2<N>$ to $S_0^2=0.85$.

**Table 1**
Structural parameters and fit goodness for Pd-foil and naked Pd nanoparticles of different sizes obtained from fits based on the too simplistic assumption that Pd local structure in nanoparticle can be modeled by a single-term contribution.

| Sample | Single shell fit results | | | | | |
|---|---|---|---|---|---|---|
| | $<R_{Pd-Pd}>$, Å | $S_0^2$ | $<N>$ | $\sigma^2$, Å$^2$ | $e_0$, eV | $\chi_\nu^2$ |
| Pd foil | $2.74\pm0.01$ | 0.85 | | $0.0058\pm1\times10^{-4}$ | $-4.4\pm0.5$ | 12.91 |
| Pd/SiO$_2$ ($D=10.5$ nm) | $2.74\pm0.01$ | | $11.0\pm0.5$ | $0.0071\pm1\times10^{-4}$ | $-4.1\pm0.5$ | 21.76 |
| Pd/Al$_2$O$_3$ ($D=3.6$ nm) | $2.74\pm0.01$ | | $9.7\pm0.5$ | $0.0079\pm1\times10^{-4}$ | $-4.2\pm0.5$ | 23.79 |
| Pd/SiO$_2$ ($D=2.8$ nm) | $2.74\pm0.01$ | | $8.5\pm0.5$ | $0.0081\pm1\times10^{-4}$ | $-4.3\pm0.5$ | 23.83 |
| Pd/Al$_2$O$_3$ ($D=1.3$ nm) | $2.73\pm0.01$ | | $6.3\pm0.5$ | $0.0092\pm1\times10^{-4}$ | $-4.8\pm0.5$ | 61.56 |

Table 1 shows the strong decrease of the mean coordination number $<N>$ for Pd in nanoparticles of $D = 1.3$ nm compared to Pd foil *fcc* structure, and a small contraction of the mean interatomic Pd–Pd distance $<R_{Pd-Pd}>$ of $\leq 0.02$ Å compared to $R_{Pd-Pd}$ in Pd foil (2.7506 Å [30]) under the small changes of variable energy parameter $e_0$ [29]. The obtained stability of $<R_{Pd-Pd}>$ upon the size of nanoparticles confirms the corresponding results of [26] and is consistent with the high stability of lattice structure parameters obtained by XRD measurements for Pd nanoparticles of sizes between 7 and 23 nm [22]. The significant decrease of $<N>$, usually associated with the contribution of large amount of the surface atoms in nanoparticles of size $\sim 2$–3 nm, is in contradiction with the minor change in $<R_{Pd-Pd}>$. According to the available crystallographic data for bulk metals, the diminishing of the coordination number from 12 to 8, 6 and 4 is connected with approximately 2%, 4% and 12% diminishing of metal–metal distances respectively [31]. One can also see the increase of parameter $\sigma^2$ followed by degradation of the fit quality (characterized by the reduced square deviation $\chi_\nu^2$ [32]) with the decrease of the nanoparticles size. This indicates that the single-term approximation used in the fit for the description of Pd environment in these nanoparticles may be inappropriate because of the increasing asymmetry and the broadening of the first peak in $|F(R)|$. At the constant room temperature and the negligible anharmonicity in the Pd–Pd motion, this is probably caused by the presence of different species of local structure of the absorbing Pd atom in nanoparticle and the possible static disorder in each of these species.

Improvement in the fit quality can be obtained by the model of Palladium nanoparticles atomic structure which enables to consider different species of the absorbing Pd atom, providing simultaneously the observed behavior of $F(R)$ in the extended $R$-range of Fig. 1(b) and the minor changes in the Pd K-edge x-ray absorption near edge structure (XANES) compared to that in Pd-foil. The simplest model for this could be the atomic cluster of a chosen size, with *fcc* structure up to the cluster's surface. However, on the real surface and in the few following atomic layers the concentration of defects increases and as the next approximation it is reasonable to assume that the model of palladium nanoparticles atomic structure should consist of the *fcc* interior region (core) and the near-surface region, which includes the atoms of the surface and subsurface layers. The last one should be a more or less distorted *fcc* structure with regard to atom positions and lattice vibrations. According to this model one must consider the following species (states) of the absorbing Pd atoms in nanoparticle, schematically illustrated in Fig. 2: Pd(1) – atoms in the core region, which have the local structure similar to that of *fcc*, as in Pd foil, and Pd(2) – atoms in the surface and subsurface layers, which we shall call as the near-surface region of nanoparticles.

According to this structural model the fit of $F(R)$ of Pd K-edge EXAFS in Palladium nanoparticles was performed by the function $\chi_{model}(k)$ compiled of the two different terms $\chi_{Pd(1)}(k)$ and $\chi_{Pd(2)}(k)$, which represent Pd(1) and Pd(2) states respectively:

$$\chi_{model}(k) = C\chi_{Pd(1)}(k) + (1-C)\chi_{Pd(2)}(k) \qquad (1)$$

where $C$ is the percentage of Pd atoms in nanoparticle, which can be attributed to the core. To perform Pd K-edge EXAFS analysis of Palladium nanoparticles atomic structure using this model, the following scheme of FT of experimental spectra and the fitting technique were used.

1. The first was the choice of the $k_{min}$ for FT at $\sim 6.5$ Å$^{-1}$ ($E \sim 24525$ eV), which enabled to reduce the influence of photoelectrons MS processes (see Fig. 3). The reduction of MS processes is especially important when the fit is performed by the complicated structural models since the presence of such contributions in the experimental signal $\chi^{experim}(k)$, not
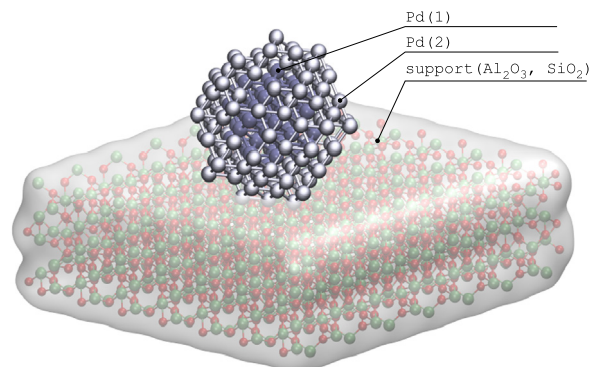


**Fig. 2.** Different states of Pd atoms in nanoparticle on Al$_2$O$_3$ and SiO$_2$ as supports: Pd(1) – atoms in the core; Pd(2) – atoms in the near-surface region.
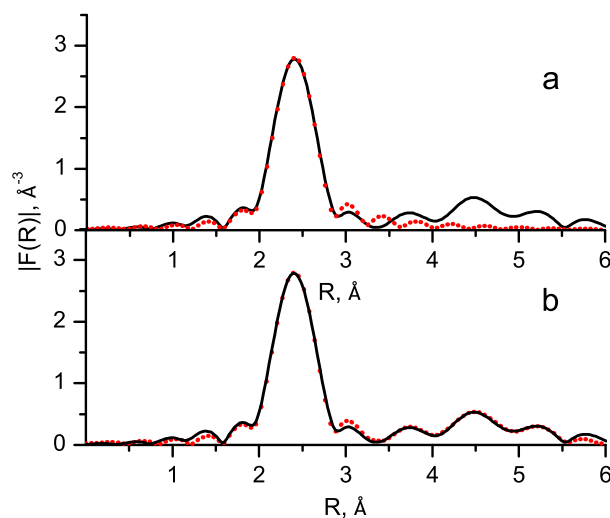


**Fig. 3.** FT magnitudes $|F(R)|$ obtained with $k_{min} = 6.5$ Å$^{-1}$ and $k_{max} = 14.0$ Å$^{-1}$. Solid black curves – $|F(R)|$ for $k^2\chi(k)$ of experimental Pd K-edge EXAFS in Pd foil; dotted red curves – results of the fits based on different approximations for Pd local structure in Pd foil: (a) only one shell around the absorbing Pd is considered (single shell approximation), (b) four nearest shells of Pd are included within the single-scattering approximation. (For interpretation of the references to color in this figure legend, the reader is referred to the web version of this article.)

considered within the fitting model, results in the increase of correlations between parameters and ambiguities in their values.

For Pd foil as the reference compound, we have shown that this $\Delta k$ interval ($k_{min} \sim 6.5$ Å$^{-1}$ and $k_{max} \sim 14.0$ Å$^{-1}$, the last was reduced to its value for Palladium nanoparticle with $D = 1.3$ nm) yielded the value of the DW parameter $\sigma^2 = 0.0058$ Å$^2$ physically reasonable for the room temperature [33,34] and the accuracy of the Pd–Pd distance, not worse than that obtained by $k_{min} = 2.5$ Å$^{-1}$. Fig. 3 compares $|F(R)|$ for $k^2\chi(k)$ of experimental Pd K-edge EXAFS in Pd foil, obtained for $\Delta k$ interval with $k_{min} \sim 6.5$ Å$^{-1}$, to those of the single-shell fit (a) and of the fit, which takes into account the first four coordination shells around the absorbing Pd atom, where each shell was represented by a single-scattering path (b). Including the second – fourth shells had no influence on the stability of the structural parameters for the first shell in Pd foil and illustrates the negligibility of the MS processes in this $\Delta k$ interval.

Using the results of [35] on the applicability of the existing criteria for signal frequencies resolution to the problem of close interatomic distances determination by FT and fitting techniques applied to energy restricted X-ray absorption spectra, the similar analysis was performed for the chosen $\Delta k$ interval from

$k_{min} \sim 6.5$ Å$^{-1}$ to $k_{max} \sim 14$ Å$^{-1}$. This $\Delta k$ is of two times longer than that considered in [35] and the obtained results show that the two models of Pd local structure can be distinguished if the difference in Pd–Pd distances is larger than $\sim 0.015$ Å, independently of the value of the ratio of amplitudes, which characterize the contributions of these models.

One more advantage of using the truncated $\Delta k$ interval is the decrease of the influence of Pd atoms bonding with oxygen atoms of the support on the determined Pd–Pd parameters. This is explained by the reduced contribution of Pd–O backscattering amplitudes in the higher $k$-range and was confirmed by FT analysis of the simulated function $\chi_{model}(k)$ compiled as a sum of experimental one $\chi_{Pd-foil}^{experim}(k)$ of Pd foil and calculated by FEFF8 [36] Pd–O contribution $\chi_{Pd-O}^{theor.}(k)$ from four oxygen atoms, with a Pd–O bond length of 2.65 Å (Fig. A1, Appendices).

2. One of the main problems in the structural analysis of Palladium nanoparticles by the considered fitting model was the strong correlations between the variable amplitude parameters, which result in instabilities and ambiguities of their values, making impossible the choice of the structural model by $\chi_\nu^2$ or F-test [37]. To reduce these correlations, the technique was applied based on the use of interdependencies of all of the correlating amplitude parameters of the signal (or $m$-dimensional surfaces, where $m$ is the number of correlating parameters), which were obtained at different weights $k^n$ and at different $\Delta k$ intervals. In this approach, the region of the parameters stability, which corresponds to minimal correlations among them, was chosen as the result of the crossing of these $m$-dimensional surfaces, where each surface corresponds to the defined values of $\Delta k$ interval and of the weight $k^n$ ($n = 1, 2, 3$).

These surfaces were obtained by systematic variation of the correlating parameters, ensuring that all possible structural models (including the ones, which give not the best fit quality, but provide the values of variable parameters in their physically reasonable boundaries) are included into the comparative analysis. The stepped variation of parameters was done by the generated code IncrementalFIT, which enabled repeated triggering of FEFFIT with step-wise change of some of the input parameters.

3. The stability of the obtained values of parameters was also improved by using a fixed contribution $\chi_{Pd-foil}^{experim}(k)$ for the first term in (1), which was obtained from experimental Pd K-edge EXAFS in Pd foil and hence, contained the exact contribution from the first and more distant shells of a Pd(1) atom in the core of nanoparticle. The inclusion of $\chi_{Pd-foil}^{experim}(k)$ as a fixed contribution into the fit by FEFFT can be easily done via small replacements in the input file feff000i.dat which contains the photoelectron backscattering amplitudes and phase shifts [32], where the number $i$ must correspond to Pd(1). In this scheme, the function $\chi_{Pd(1)}(k)$ in (1) was constructed as $\chi_{Pd(1)}(k) = \chi_{Pd-foil}^{experim}(k)\exp(-2\Delta\sigma_{Pd(1)}^2 k^2)$. The factor $\exp(-2\sigma_{Pd(1)}^2 k^2)$ takes into account the difference in

structural order in the first shell of an atom in a nanoparticle with that of a one in the foil. $\Delta\sigma_{Pd(1)}^2$ for Pd foil equals zero by definition. In the sequel, if the obtained values of $\Delta\sigma_{Pd(1)}^2$ will be negligible, then it will confirm the made assumption on $fcc$ structure for the core of Palladium nanoparticles. Otherwise, the noticeable or large values of $\Delta\sigma_{Pd(1)}^2$ ($> 0.001$ Å$^2$) will indicate that the $fcc$ structure is either distorted or the fit does not require the function $\chi_{Pd-foil}^{experim}(k)$ and our assumption on $fcc$ core is wrong. It must be noted also, that the only variable parameter in the used construction for the contribution of the core region was $\Delta\sigma_{Pd(1)}^2$. Therefore backscattering amplitudes and phase shifts for this term were not needed within the fit and hence, additional energy variable parameter like $e_0(Pd(1))$ was not used for this contribution.

## 3. Results of atomic level description of palladium nanoparticles and discussion

For Palladium nanoparticles of sizes $D = 1.3$, 2.8, 3.6 and 10.5 nm on Al$_2$O$_3$ and SiO$_2$ as supports the fit of $F(R)$ of experimental Pd K-edge EXAFS was performed by (1) using the technique of Section 2 with $k_{min} \sim 6.5$ Å$^{-1}$, the global variable $C$ and variable $\Delta\sigma_{Pd(1)}^2$ for the term $\chi_{Pd(1)}(k)$. The contribution of the near-surface Pd(2) atoms was given in (1) by the function $(1-C)\chi_{Pd(2)}(k)$, where $\chi_{Pd(2)}(k)$ was approximated by the single-shell term, taken in the single-scattering form [29] with the average structural parameters: $<N_{Pd(2)}>$ – mean number of nearest neighbors for Pd(2) atom, $\sigma_{Pd(2)}^2$ – mean DW parameter for Pd(2)–Pd(2) interaction, $<R_{Pd(2)-Pd(2)}>$ – mean interatomic distance between nearest Pd(2) atoms and energy parameter $e_0(Pd(2))$. The correlation of amplitude parameters $C$, $\Delta\sigma_{Pd(1)}^2$, $<N_{Pd(2)}>$, $\sigma_{Pd(2)}^2$ was reduced by the technique of Section 2, applying it to $F(R)$ obtained for: (i) differently weighted oscillatory parts $k^n\chi(k)$ ($n = 1, 2, 3$) of Pd K-edge EXAFS and for (ii) different $(\Delta k)_i$ intervals ($i$ numbers the intervals with $k_{min}$ changed from 6.0 to 7.5 Å$^{-1}$ and $k_{max}$ changed from 13.0 to 14.0 Å$^{-1}$). For each of these $F(R)$ functions the fit was performed by the stepped variation of parameters $C$ (from 0.00 to 1.00, step 0.01), $\Delta\sigma_{Pd(1)}^2$ (from 0.0000 to 0.0070 Å$^2$, step 0.0001), $<N_{Pd(2)}>$ (from 1.0 to 12.0, step 0.1) and varying one amplitude parameter $\sigma_{Pd(2)}^2$ and parameters $<R_{Pd(2)-Pd(2)}>$, $e_0(Pd(2))$. As a result, we have obtained the set of four-dimensional surfaces $\{\sigma_{Pd(2)}^2(C, \Delta\sigma_{Pd(1)}^2, \langle N_{Pd(2)}\rangle)\}_{k^n,(\Delta k)_i}$, where each surface corresponds to one defined value of $k^n$ and $(\Delta k)_i$. The crossing region of these surfaces corresponds to the reduced correlation between the four amplitude parameters, and was determined by the unbiased sample dispersion [38] of $\sigma_{Pd(2)}^2$ with an accuracy to $\sim 0.0005$ Å$^2$.

Determining the values of correlating amplitude parameters by this scheme and employing the fitting technique of Section 2, reduced significantly any ambiguity, improved their stability and

**Table 2**
Structural Pd–Pd parameters for the core and for the near-surface regions in naked Palladium nanoparticles of different sizes on supports Al$_2$O$_3$ and SiO$_2$, determined by the used fitting technique.

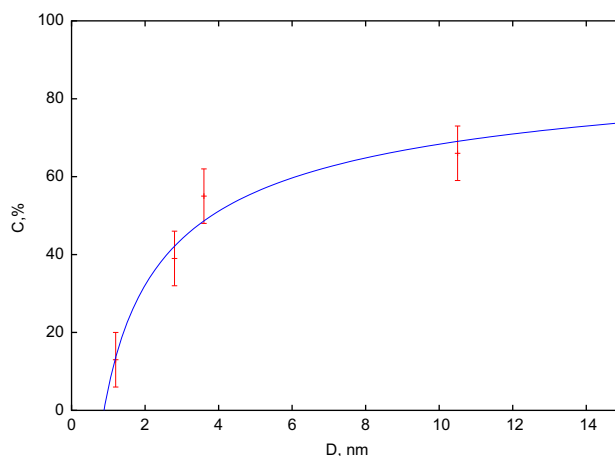| Pd nanoparticles on the supports | Core region of Pd nanoparticle | | Near-surface region of Pd nanoparticle | | | | |
|---|---|---|---|---|---|---|---|
| | $C$ | $\Delta\sigma_{Pd(1)}^2$, Å$^2$ | $<N_{Pd(2)}>$ | $\sigma_{Pd(2)}^2$, Å$^2$ | $<R_{Pd(2)-Pd(2)}>$, Å | $e_0(Pd(2))$, eV | $\chi_\nu^2$ |
| Pd (10.5 nm)/SiO$_2$ | $0.66 \pm 0.07$ | 0.0004 | $10.3 \pm 0.5$ | $0.0085 \pm 1 \times 10^{-4}$ | $2.75 \pm 0.015$ | $-3.5 \pm 0.1$ | 9.1 |
| Pd (3.6 nm )/Al$_2$O$_3$ | $0.55 \pm 0.07$ | 0.0005 | $9.1 \pm 0.5$ | $0.0107 \pm 1 \times 10^{-4}$ | $2.76 \pm 0.015$ | $-2.8 \pm 0.5$ | 10.2 |
| Pd (2.8 nm)/SiO$_2$ | $0.39 \pm 0.07$ | 0.0007 | $6.5 \pm 0.5$ | $0.0089 \pm 1 \times 10^{-4}$ | $2.74 \pm 0.015$ | $-3.2 \pm 0.5$ | 8.7 |
| Pd (1.3 nm)/Al$_2$O$_3$ | $0.13 \pm 0.07$ | 0.0010 | $6.1 \pm 0.5$ | $0.0110 \pm 1 \times 10^{-4}$ | $2.73 \pm 0.015$ | $-5.1 \pm 0.5$ | 25.1 |
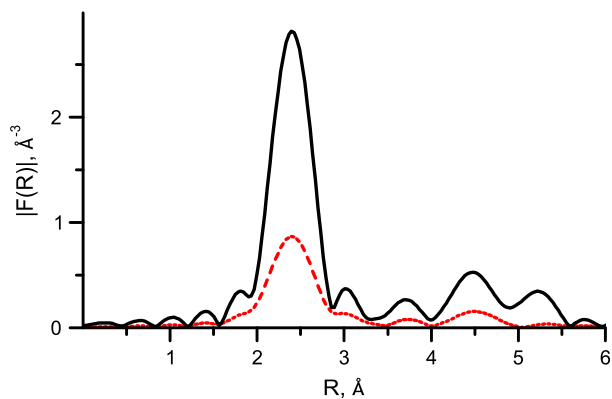
**Fig. 4.** $|F(R)|$ of the function $k^2\chi_{Pd(1)}(k)$ calculated for the absorbing Pd(1) atoms of the undistorted *fcc* interior region of Palladium cluster with radius $\sim 6.0$ Å (solid black curve) and of the $k^2\chi_{Pd(2)}(k)$ calculated for the absorbing Pd(2) atoms of the cluster's surface, under the variation of $\sim 0.05$ Å in the nearest neighbors Pd(2)–Pd(2) distances (dashed red curve). (For interpretation of the references to color in this figure legend, the reader is referred to the web version of this article.)



**Fig. 5.** Percentage ($C$) of the total number of Pd atoms in Pd nanoparticle, which have the same local structure as in *fcc* structure of Pd foil, as a function of size ($D$). Results of the FT analysis of Pd K-edge EXAFS (red points) are approximated by the solid blue curve, obtained by Eq. (3). (For interpretation of the references to color in this figure legend, the reader is referred to the web version of this article.)

provided the choice of nanoparticles structural model by $\chi_\nu^2$ and *F*-test values. Corresponding Pd–Pd structural parameters are presented in Table 2.

The very low values of $\Delta\sigma_{Pd(1)}^2$ together with the results of comparison of $|F(R)|$ in the extended *R*-range in Fig. 1 (b) unambiguously indicate that irrespectively of nanoparticles size, Pd atoms in the core region have the local structure which corresponds to the *fcc* structure of Pd-foil. One can see also that the mean Pd(2)–Pd(2) distance in the near-surface region is slightly shortened in the smaller particles, while for the larger sizes it is very close or approximately equal to that of the core within the above mentioned accuracy of $\sim 0.015$ Å for interatomic distances resolution by the used $\Delta k$ interval. Nevertheless, for nanoparticles of size 2.8 nm and larger the amplitude parameters of the near surface region can be also distinguished from those of the core due to the existed *a priori* difference in the DW parameters values for these regions.

To illustrate this possibility and to validate the values of amplitude parameters presented in Table 2, we have performed the FT analysis of the simulated functions $\chi(k)=C\chi_{Pd-foil}^{experim}(k)\exp(-2\Delta\sigma_{Pd(1)}^2 k^2)+(1-C)\chi_{Pd(2)}(k)$. The last term in this expression was calculated by averaging the contributions of the near-surface Pd(2) atoms in Palladium cluster with *fcc* structure truncated at $\sim 6.0$ Å, the core value 2.75 Å for $<R_{Pd(2)-Pd(2)}>$, but at various values of $\sigma_{Pd(2)}^2$ (from 0.008 to 0.012 Å$^2$), $<N_{Pd(2)}>$ (from 6.0 to 11.0) and $C$ (from 0.1 to 1.0). The fit of $F(R)$ of these functions, performed by the model with two terms (where the first term represents the core and the second – the near-surface region) enabled to recover the used parameters of the term $(1-C)\chi_{Pd(2)}(k)$ with the following accuracies: $\sigma_{Pd(2)}^2 \pm 0.001$ Å$^2$, $C \pm 0.07$ and $<N_{Pd(2)}> \pm 0.5$, for the ranges of their values presented in Table 2. However, the estimate of the boundary values of $\sigma_{Pd(2)}^2$, $<N_{Pd(2)}>$ and $C$ which can be distinguished against the background of the core contribution $C\chi_{Pd-foil}^{experim}(k)\exp(-2\Delta\sigma_{Pd(1)}^2 k^2)$ under the close values of $R_{Pd-Pd}$ for the core and the near surface regions requires additional study.

The accuracy of $C$, determined from experimental Pd K-edge EXAFS in nanoparticles is $\sim 7\%$ (using the $S_0^2$ value of the reference Pd foil) and cannot be improved because of remaining correlations between $C$ and $\sigma_{Pd(2)}^2$. Meanwhile, for each size of nanoparticles, the values of mean structural parameters $<N_{Pd(2)}>$ and $<R_{Pd(2)-Pd(2)}>$, as well as the value of energy parameter $e_0(Pd(2))$ for the

near-surface region, exhibited remarkable stability, independent of the inaccuracies in $C$ determination.

The values of parameters $\sigma_{Pd(2)}^2$ for the near-surface region, presented in Table 2, are noticeably larger than the value of DW-parameter for the core (0.0058 Å$^2$). This indicates that there is a significant variation in the Pd(2)–Pd(2) distances in the near-surface region of Palladium nanoparticles. Such variations were modeled by calculating the averaged contribution $\chi_{Pd(2)}(k)$ from the absorbing Pd(2) atoms located at the nonequivalent surface positions in Palladium cluster with radius of $\sim 6.0$ Å. This cluster had the undistorted *fcc* structure for the interior atoms, but the local structure in the vicinity of the absorbing Pd(2) atoms of the surface was distorted so that the changes in interatomic distances between the Pd(2) atom and its nearest neighbors did not exceed $\sim 0.2$ Å. Calculations of $\chi_{Pd(2)}(k)$ were performed by FEFF8 using the same approximation for the photoelectrons scattering processes as that used for the dashed red curve of Fig. 3(b). Fig. 4 compares $|F(R)|$ of the function $k^2\chi_{Pd(2)}(k)$ calculated for the absorbing Pd(2) atoms of the cluster's surface under the variation of $\sim 0.05$ Å in the nearest neighbors Pd(2)–Pd(2) distances, with that calculated for the absorbing Pd(1) atoms of the undistorted *fcc* core of Palladium cluster.

Fig. 4 shows the reduction of magnitude of all peaks in $|F(R)|$ of the surface Pd(2) atoms. The performed simulations revealed that for these atoms the *fcc* behavior of $F(R)$ with the minor changes in *R*-positions of peaks in the extended *R*-range (up to $\sim 5.5$ Å) is retained under the distortions of *fcc* structure in the vicinity of the absorbing Pd(2) atom until the corresponding changes in the nearest neighbors Pd(2)–Pd(2) distances do not exceed $\sim 0.05$ Å.

Fig. 5 shows the dependence of the percentage $C$ of Pd atoms in the core of Palladium nanoparticles on their size $D$. This dependence $C(D)$ is well described by the so-called "cluster size equation" [39]:

$$C(D)=C(\infty)-A\left(\frac{2R_0}{D}\right)^{3\beta} \qquad (3)$$

where $C(\infty)=100\%$ is the percentage of core atoms in bulk compound, $R_0=0.275/2$ nm is the Van der Waals radius of the Pd atom, $A$ and $\beta$ are two dimensionless adjustable parameters. The continuous curve $C(D)$ of Fig. 5 was obtained by the fitted values $A=170 \pm 20$ and $\beta=0.16 \pm 0.02$, where the last one is in its reasonable boundaries $0 < \beta \leq 1$.

The size $D$ of a nanoparticle, at which the value of $C$ vanishes, corresponds to the case, in which the core is absent, so that all the atoms remain in the near-surface region. Using the curve $C$ ($D$) of Fig. 5 and making the assumption that the thickness ($d$) of the near-surface layer of nanoparticle negligibly changes with varying size $D$, one can estimate the thickness of this shell to be $d \approx 0.44 \pm 0.08$ nm.

## 4. Conclusions

The study of features formation in the extended $R$-range of $|F(R)|$ of Pd K-edge EXAFS in Pd foil and determination of atomic structure in Palladium nanoparticles of sizes between 1.3 and 10.5 nm, on $Al_2O_3$ and $SiO_2$ as support was performed by experimental Pd K-edge EXAFS, the used scheme of FT and the fitting technique for the processing of these spectra. The following conclusions can be made:

- if the FT of experimental Pd K-edge EXAFS in Pd foil is performed by $k_{min} \sim 6.5$ Å$^{-1}$ ($E \sim 24{,}518.5$ eV) then the features of $F(R)$ in the extended $R$-range (up to $\sim 5.5$ Å) are reproduced by taking into account the photoelectron single scattering on the first four shells around the absorbing Pd atom. Thus chosen $\Delta k$ interval provides the same accuracy of the first shell Pd–Pd structural parameters in Pd foil as the extended interval with $k_{min} = 2.5$ Å$^{-1}$, but reduces the effect of photoelectron MS processes – one of the main origins of strong correlations between amplitude parameters of the fit;
- the used scheme of FT and the fitting technique of $F(R)$ of experimental spectra enabled to overcome instabilities of the obtained values of structural parameters and to go beyond the averaged description of Palladium nanoparticles structure to more detailed characterization, which includes determination of the atomic structure of their core and the mean structural parameters of the near-surface region;
- the local structure of Pd atoms in the core region of nanoparticles is similar to that of the *fcc* structure of bulk Pd, irrespective of size. The percentage ($C$) of the total number of Pd atoms, which can be attributed to the core, basically follows the particles size ($D$). The determined dependence $C(D)$ is well described by the "cluster size equation" with two adjustable parameters;
- $|F(R)|$ of the average contribution of the absorbing Pd (2) atoms of the surface region of Palladium cluster with *fcc* structure differ from that of Pd(1) of the core by significant (up to $\sim$ two times) reduction in the magnitudes of peaks under their stable positions and the conserved general form of $|F(R)|$ in the extended $R$-range. The distortions of *fcc* structure in the vicinity of the absorbing Pd (2) atom retains this conclusion until the corresponding changes in the nearest neighbors Pd(2)–Pd(2) distances do not exceed $\sim 0.05$ Å;
- in the near-surface region of Palladium nanoparticle, nearest-neighbors Pd(2)–Pd(2) distances show a large DW-parameters and the averaged bond length slightly contracted for nanoparticles of sizes $\sim 1.5$ nm. No Pd–Pd distances or scattering paths, clearly distinguished from those in *fcc* core, are found for the near-surface region of nanoparticles. The distribution of Pd–Pd distances in the near-surface region of Pd nanoparticles on $Al_2O_3$ as support is bigger than that on $SiO_2$.
- The suggested technique of the fit is particularly promising for identification of the core-shell structure in noble and transition atoms bimetallic nanoparticles on the supports.

## Appendices

*Simulation of interaction of the surface Pd atoms with O atoms of the support*

Fig. A1 compares $|F(R)|$ of $\chi_{model}(k) = \chi_{Pd-foil}^{experim}(k) + \chi_{Pd-O}^{theor.}(k)$ with that of the single-shell Pd–Pd fit, where FT was performed over the extended $\Delta k$ interval ($k_{min} = 2.5$ Å$^{-1}$; $k_{max} = 14.0$ Å$^{-1}$) and over the truncated one with $k_{min} = 6.5$ Å$^{-1}$. The use of the $\Delta k$ with $k_{min} = 6.5$ Å$^{-1}$ simplifies the shape of the main peak in $|F(R)|$ removing its features on the left shoulder, and corresponding fit gives the same values of Pd–Pd structural parameters for the first shell of Pd as those in Pd foil presented in Table 1.
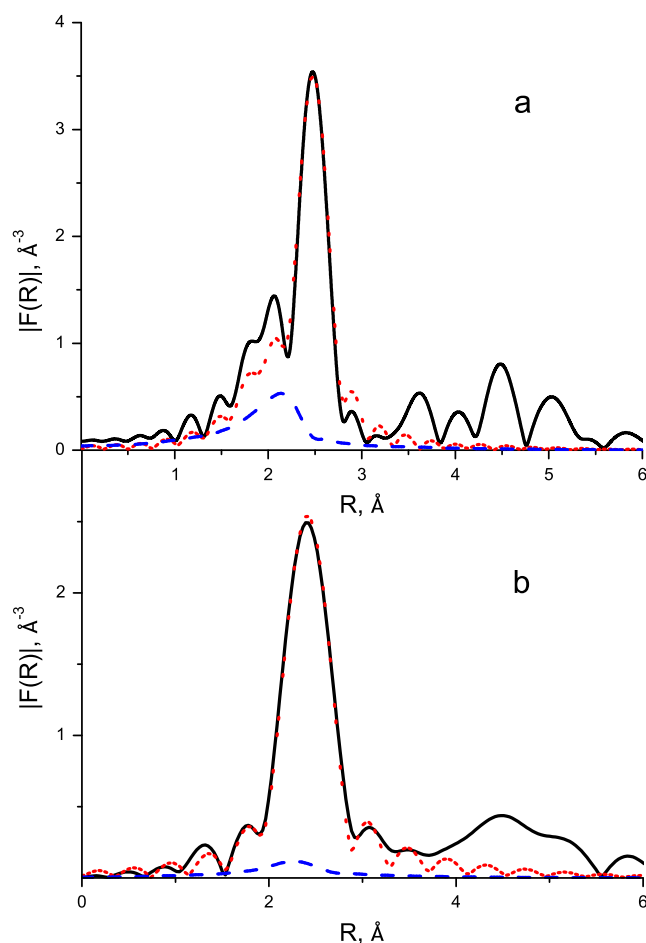


**Fig. A1.** Comparison of FT magnitudes $|F(R)|$ of $k^2\chi_{mod\ el}(k)$, where $\chi_{mod\ el}(k) = \chi_{Pd-foil}^{experim}(k) + \chi_{Pd-O}^{theor.}(k)$ (solid black curves) obtained: (a) by the extended $\Delta k$ interval ($k_{min} = 2.5$ Å$^{-1}$, $k_{max} = 14.0$ Å$^{-1}$) and ( b) by the truncated one ($k_{min} = 6.5$ Å$^{-1}$, $k_{max} = 14.0$ Å$^{-1}$) with corresponding functions of the single-shell Pd–Pd fit (dotted red curves). Dashed blue curves show the magnitude of Pd–O contributions within the used $\Delta k$ intervals. (For interpretation of the references to color in this figure legend, the reader is referred to the web version of this article.)

# References

[1] L. Jinlin, L. Shanfu, W. Deli, Y. Meng, L. Zili, X. Changwei, San Ping Jiang, Electrochim. Acta 54 (2009) 5486–5491.

[2] L. Fengli, C. Jing, C. Jingla, San Ping Jiang, H. Tianmin, P. Jian, L. Jian, Electrochem. commun. 10 (2007) 42–46.

[3] F. Kadirgan, S. Beyhan, T. Atilan, Int. J. Hydrogen Energy 34 (2009) 4312–4320.

[4] D. Astruc, Inorg. Chem. 46 (2007) 1884–1894.

[5] J. Zhang, Y. Mo, M.B. Vukmirovic, R. Klie, K. Sasaki, R.R. Adzic, J. Phys. Chem. B. 108 (2004) 10955–10964.

[6] C.C. Cassol, A.P. Umpierre, G. Machado, S.I. Wolke, J. Dupont, J. Am. Chem. Soc. 127 (2005) 3298–3299.

[7] S.I. Sanchez, L.D. Menard, A. Bram, Joo H. Kang, M.W. Small, R.G. Nuzzo, A.I. Frenkel, J. Am. Chem. Soc. 131 (2009) 7040–7054.

[8] S. Jagdeep, C. Lamberti, J.A. van Bokhoven, Chem. Soc. Rev. 39 (2010) 4754–4766.

[9] S. Bordiga, E. Groppo, G. Agostini, J.A. van Bokhoven, C. Lamberti, Chem. Rev. 113 (2013) 1736–1850.

[10] R. Litrán, B. Sampedro, T.C. Rojas, M. Multigner, J.C. Sánchez-López, P. Crespo, C. López-Cartes, M.A. García, A. Hernando, A. Fernández, Phys. Rev. B. 73 (2006) 054404–054410.

[11] P.J. Ellis, J.S. Fairlamb Ian, S.F.J. Hackett, K. Wilson, A.F. Lee, Angew. Chem. 49 (2010) 1820–1824.

[12] S. Takafumi, R. Prins, J. Phys. Chem. B 102 (1998) 8426–8435.

[13] A.I. Boronin, E.M. Slavinskaya, I.G. Danilova, R.V. Gulyaev, Amosov Yul, P. A. Kuznetsov, I.A. Polukhina, S.V. Koscheev, V.I. Zaikovskii, A.S. Noskov, Catal. Today 144 (2009) 201–211.

[14] X. Bin, C. Ping, H. Qi, L. Jianyi, L.T. Kuang, J. Mater. Chem. 11 (2001) 2378–2381.

[15] J.A. McCaulley, J. Phys. Chem. 97 (1993) 10372–10379.

[16] R.J. Davis, S.M. Landry, J.A. Horsley, M. Boudart, Phys. Rev. B 39 (1989) 10580–10583.

[17] K. Takeshi, K. Yoshinori, A. Kiyotaka, I. Yasuhiro, Chem. Soc. Jpn. 72 (1999) 673–681.

[18] Y.-F. Han, D. Kumar, D.W. Goodman, J. Catal. 230 (2005) 353–358.

[19] M.A. Newton, Carolina Belver-Coldeira, Arturo Martínez-Arias, Marcos Fernández-García, Nat. Mater. 6 (2007) 528–532.

[20] S. Yuan, A.I. Frenkel, R. Isseroff, C. Shonbrun, M. Forman, S. Kwanwoo, K. Tadanori, H. White, Z. Lihua, Z. Yimei, M.H. Rafailovich, J.C. Sokolov, Langmuir 22 (2005) 807–816.

[21] G. Agostini, R. Pellegrini, G. Leofanti, L. Bertinetti, S. Bertarione, E. Groppo, A. Zecchina, C. Lamberti, J. Phys. Chem. C 113 (2009) 10485–10492.

[22] L. Chih-Ming, H. Tsu-Lien, H. Yen-Heng, W. Kung-Te, T. Mau-Tsu, L. Chih-Hao, C.T. Chen, Y.Y. Chen, Phys. Rev. B 75 (2007) 125426–125431.

[23] O.A. Belyakova, Y.V. Zubavichus, I.S. Neretin, A.S. Golub, Yu.N. Novikov, E.G. Mednikov, M.N. Vargaftik, I.I. Moiseev, Yu.L. Slovokhotov, J. Alloys Compd. 382 (2004) 46–53.

[24] K. Vijay, K. Yoshiyuki, Phys. Rev. B 66 (2002) 144413–144423.

[25] T. Teranishi, M. Miyake, Chem. Mater 10 (1998) 594–600.

[26] W.T. Min, J.T. Miller, J.A. van Bokhoven, J. Phys. Chem. C 113 (2009) 15140–15147.

[27] M. Newville, B. Ravel, D. Haskel, J.J. Rehr, E.A. Stern, Y. Yacoby, Physica B 208–209 (1995) 154–156.

[28] E.D. Crozier, J.J. Rehr, R. Ingals, Amorphous and liquid systems, in: D.C. Koningsberger, R. Prins (Eds.), X-Ray Absorption. Principles, Applications, Techniques of EXAFS, SEXAFS and XANES, Wiley & Sons, New York, 1998, pp. 373–442.

[29] E.A. Stern, Theory of EXAFS, in: DC Koningsberger, R Prins (Eds.), X-Ray Absorption. Principles, Applications, Techniques of EXAFS, SEXAFS and XANES, J. Wiley & Sons, New York, 1998, pp. 3–51.

[30] R.W.G. Wyckoff, Crystal StructuresWiley & Sons, New York (1963) 10.

[31] Cambridge structural database system. Version 5.22. Cambridge Crystallographic Data Centre. 2001.

[32] M. Newville, IFEFFIT Web Page and On-line Documentation, ⟨http://cars9.uchicagj.edu/ifeffit⟩.

[33] A.V. Poirkova, J.J. Rehr, Phys. Rev. B 59 (1999) 948–957.

[34] Y. Nishihata, J. Mizuki, T. Akao, H. Tanaka, M. Uenishi, M. Kimura, T. Okamoto, N. Hamada, Nature 418 (11) (2002) 164–167.

[35] L.A. Bugaev, L.A. Avakyan, V.V. Srabionyan, A.L. Bugaev, Phys. Rev. B 82 (2010) (064204–1–9).

[36] L. Ankudinov, B. Ravel, J.J. Rehr, S.D. Conradson, Phys. Rev. B. 58 (1998) 7565.

[37] L. Downward, C.H. Booth, W.W. Lukens, F. Bridges, A variation of the F-test for determining statistical relevance for particular parameters in EXAFS analysis, in: X-Ray Absorption Fine Structure XAFS13: 13th International Conference, July 9–13, 2006. AIP Conference Proceedings, LBNL-62566, vol. 882, 2007, p. 129.

[38] D.C. Montgomery, G.C. Runger, Applied Statistics and Probability for Engineers, J. Wiley & Sons, New York (1994) 201.

[39] J. Jortner, Z. Phys. D Atoms: Mol. Clusters 24 (1992) 247–275.